Tissue libraries enable rapid determination of conditions that preserve antibody labeling in cleared mouse and human tissue

Theodore J. Zwang, Rachel E. Bennett, Maria Lysandrou, Benjamin Woost, Anqi Zhang, Charles M. Lieber, Douglas S. Richardson, Bradley T. Hyman

Abstract

Difficulty achieving complete, specific, and homogenous staining is a major bottleneck preventing the widespread use of tissue clearing techniques to image large volumes of human tissue. In this manuscript we describe a procedure to rapidly produce immunostaining protocols for antibody labeling of cleared brain tissue. We prepared libraries of 500-1000 µm thick tissue sections that are fixed, pre-treated, and cleared via different procedures and then used to optimize staining conditions for a panel of antibodies. Results from a library of mouse tissue correlate well with results from a similarly prepared library of human brain tissue, suggesting mouse tissue is an adequate substitute for protocol optimization. These data show that procedural differences do not influence every antibody-antigen pair in the same way, and minor changes can have deleterious effects, so optimization should be conducted for each target. The approach outlined here will help guide researchers to successfully label a variety of targets, thus removing a major hurdle to accessing the rich 3D information available in large, cleared human tissue volumes.

Introduction

In recent years, there have been substantial improvements in the techniques used to visualize features of brains, organs, and whole organisms in three dimensions. One promising method, tissue clearing, involves lipid removal and refractive index matching to significantly decrease light scattering. Tissue clearing allows for light microscopy to observe the distribution of individual molecules throughout entire organs millimeters to centimeters in size.[1,2] This holds extraordinary promise for understanding human diseases, where the identification and characterization of abnormal structures is often an early step towards the development of clinical treatments.[3] Difficulties with antibody staining and labeling is common in traditional thin tissue section histology, but is dramatically amplified in large, cleared samples. Although techniques have been developed to improve the homogeneity of staining (SWITCH[4]) and increase the speed of antibody labeling in large, cleared tissue (eFlash[5], EFIC[6], MDH[7]), these methods only work if an antibody's epitope is well preserved during the tissue preparation and clearing process. This is rarely the case and complete, specific and homogenous staining is now the most common bottleneck preventing the widespread use of tissue clearing in samples that cannot be modified to express fluorescent proteins, especially human tissue. Additionally, much of this work has been optimized for studies in rodents, and only a few recent studies apply tissue clearing techniques to human tissue.[8-12] Here, we present a simple optimization strategy and automated analysis routine that allows researchers to tune their immunohistochemistry protocols for labeling protein targets in cleared and uncleared brain tissue. Further, we demonstrate that our optimized protocols can be extended from mouse to human tissue.

Immunohistochemistry (IHC) has a history of being difficult, with myriad improvements taking place over decades to allow for its current ubiquity in pathology laboratories and biomarker discovery.[11] The basic concept of IHC is to use antibodies to label specific antigens in tissue, which can then be imaged to

determine their distribution throughout tissue. Successful IHC requires four fundamentals: 1) the antibody cannot denature, 2) the epitope cannot denature, 3) the antibody must diffuse completely through the tissue and 4) the antibody must only bind its intended target. Often researchers develop lengthy protocols that include steps thought to enable successful labeling but are not necessarily based on empirical evidence or are borrowed from others using completely different antibodies or tissues. In general, an IHC protocol first requires tissue to be fixed in place, enabling the preservation of its structure. This is typically performed by freezing the tissue or placing it in an aldehyde containing solution like formalin. It may then be stored for long periods of time before an investigation is initiated. Next, different methods of antigen retrieval can be deployed to enhance antibody binding. The tissue may also be blocked by incubating with serum or other agents to deactivate endogenous enzymes and reduce non-specific antibody staining. Finally, when labeling and imaging thick tissue, tissue clearing protocols are required and introduce several additional chemical treatments including chemical crosslinking, removal of undesired molecules from the tissue, and immersion in a solution that is refractive index matched to the processed tissue[2,13].

It is well understood that differences in staining quality results from small changes in tissue composition, individual antibodies, their epitopes, and overall tissue structure that can be induced by each step of an IHC protocol[3,11,14]. A myriad of IHC protocols exist, and it is usually possible to reproduce these protocols exactly as written with the same tissues, antibodies, and fluorophores. Unfortunately, it is common to have difficulties extending these protocols to different antibodies or tissues. And the complexity of these multi-step protocols makes it prohibitively costly and time-intensive for researchers to optimize all possible IHC conditions for their specific study. This has slowed the testing and adoption of reported improvements in IHC procedures.

Experiments with human tissue samples are essential for a complete understanding of the pathology of many diseases. However, extensive optimization of IHC protocols in human tissue is often not possible due to its scarcity. Variability across protocols could confound results and limit the insight gained from such precious resources. Ideally, researchers could optimize protocols in a more plentiful model species such as mice and directly transfer these methods to human samples. However, it is not often clear whether IHC improvements in mice[4,15,16] would translate to better staining of human tissue. Methods that can rapidly determine optimal IHC protocols for individual antibodies and assess their applicability to tissues from different species are needed.

Inspired by previous experience troubleshooting IHC in large volumes of mouse brain tissue, we developed a practical workflow to rapidly optimize IHC protocols for different antibodies. We then applied this methodology to a variety of targets in mouse and human brain tissue to understand 1) how much variation exists if IHC protocols are optimized for individual antibodies and 2) if optimized IHC protocols can be generalized between species. We compare the effect of different IHC protocols on antibodies and a small molecule DNA label, 4’,6-diamidino-2-phenylindole (DAPI). We also test the influence of protocols on different antibodies raised against the same protein target and finally, explore whether IHC protocols optimized in mouse tissue can produce equally high-quality staining in human tissue. Together this work provides a method to empirically determine the optimal procedure for IHC studies in large volume tissue, assess its generalizability, and supports the use of abundant mouse tissue to optimize IHC protocols for scarce human samples.

Results

Strategy to rapidly assess the optimization of protocols

Our workflow for determining an optimal IHC protocol is inspired by the success of quantitative structure-activity relationship modeling (QSAR) for drug discovery. QSAR models are used to predict the biological activities of untested drugs by first testing a library of drugs with similar but varied structures, measuring how each drug affects the activity, then creating a model that relates the structural changes to the observed activities.[17] Borrowing from this strategy allows for us to predict the optimal staining protocol without needing to test every possible combination of conditions.

We created a library of cleared tissue that was processed using a variety of different protocols (Scheme 1). It is unnecessary and impractical to create this library from large intact organs such as whole mouse brains, therefore tissue sections were used. Optimizing tissue thickness is important; if the sections are too thick, extensive incubation times are required. However, if the tissue sections are too thin, the impact of antibody diffusion cannot be fully appreciated and compared across protocols. We found tissue sections 0.5-1.0 mm thick and antibody incubation times of 18-24 hours to be sufficient to assess the influence of our chosen conditions on IHC staining quality, and allows dozens of protocols or multiple antibodies to be tested with tissue from a single mouse brain depending on the epitope distribution.

To simplify our analysis, each protocol was designed to change in one way relative to another so the effect that each change in conditions has on antibody labeling can be isolated, and so IHC outcomes translate into a quantifiable metric of quality described below. With this strategy we were able to predict the optimal combination of conditions for each antibody we tested.

Measuring IHC quality in cleared tissue

To quantify the quality of IHC in these tissues we developed a data analysis pipeline that isolates objects based on the intensity of fluorescence relative to nearby background (Scheme 2). We found previous methods of cell-counting were not applicable to non-cell shapes like vasculature, and simply quantifying fluorescence intensity did not properly account for changes in background fluorescence among conditions. Assuming that the antigens have relatively constant distribution with the depth of imaging, the area of each image in a z-stack with fluorescence that has a user-defined value above background could be used as a figure of merit for staining quality across conditions.

Conditions that influence antibody and epitope preservation

Starting from a comprehensive collection of published IHC protocols,[2,3,8,13] we selected a subset of commonly varied conditions to create 12 total protocols to test as a proof of principle. Each protocol is nearly identical, only varying by a single condition to allow for a complete understanding of how each change influences staining. The baseline protocol involved minimal processing and gentle conditions. Specifically, the tissue was fixed in 4% paraformaldehyde (PFA) for 2 days post-perfusion, embedded in hydrogel made of 4% acrylamide, delipidated in Sodium dodecyl sulfate (SDS) for 1 day at 37°C, rinsed in phosphate-buffered saline with 0.2% Triton X-100 (PBST) at 4°C, and incubated with antibodies at 4°C for 18 hours. We then created a library of tissue that was processed using small changes to this baseline protocol, so we could compare how each of these changes influenced IHC quality. This library included changes in the composition of the hydrogel (with and without 4% PFA), changes in delipidation time (1 day, 2 days, 3 days), additional steps before antibody incubation (such as unmasking with 50°C or

incubation with glycine), and differential changes in antibody incubation temperature (4°C or room temperature). In addition to this library, we also examined the effects of boiling samples in citrate buffer before or after delipidation, heating to temperatures above 70°C before immunolabeling, and removal or decrease of PFA concentration in the transcardial perfusion or post-perfusion fixing step. (Scheme 1) However, these conditions were universally observed to negatively impact IHC or tissue integrity so they were excluded from our final library.

We chose two antibodies commonly used in neuroscience studies of cleared volumes (Glut1 and NeuN) and performed IHC on the same tissue sections from a mouse cortex that were processed according the 12 protocols (figure 1). Increasing delipidation time to two days had a negative influence on NeuN staining, and a positive influence on Glut1 staining, but both showed worse IHC when increasing the delipidation time further. Incubation of tissue at 50°C for one hour prior to antibody incubation improved staining for Glut1, and had a negative effect on staining for NeuN. Glycine treatment had no significant effect on NeuN staining, but inhibited Glut1 staining. Incubating antibodies at RT improved NeuN staining but had no effect on Glut1 staining. Inclusion of PFA in the hydrogel resulted in decreased IHC quality for both Glut1 and NeuN, however this significantly improved IHC of dopamine receptor 2 (figure S5). Intriguingly, staining with DAPI appears insensitive to the different protocols (figure 2). Together, these results show that different conditions can have opposite effects on the quality of staining and depth of antibody penetration and reinforce the importance of optimizing sample preparation conditions for each antibody.

Comparison of IHC conditions for different antibodies directed against a single protein

A common strategy following unsuccessful IHC in tissue is to test antibodies from different suppliers or raised against different epitopes that label the desired target. To better understand whether optimal IHC protocols may be shared for antibodies against the same target, we compared the staining of a monoclonal GFAP with a conjugated fluorophore and a polyclonal GFAP with a secondary antibody in the same tissue. Immunolabeling GFAP with different antibodies shows that the trends in staining quality are similar for both antibodies across all conditions (figure 3). This suggests that conditions that enhance GFAP stability and prevent epitope denaturation could have a positive effect on all GFAP antibodies provided the antibodies are of high quality, have high specificity and limited off-target binding. This also suggests that IHC is limited more by denaturation of the epitope than the antibody itself. Importantly, primary antibodies with a conjugated fluorophore showed significantly better penetration, signal-to-noise ratio, and less off-target staining for both GFAP antibodies under nearly all conditions where IHC successfully labeled its target (figure 3). As this also approach reduces the length of the staining protocol, it is recommended to use primary antibodies directly conjugated to fluorophores whenever possible.

In order to examine how much of the observed variability in antibody labeling is due to targets being more or less accessible depending on cell type or subcellular location, multiple antibodies were also chosen that recognize tau protein. Tau is a microtubule associated protein that is primarily expressed by neurons and is the main component of neurofibrillary tangles in Alzheimer's disease. We chose three commonly used antibodies against tau and tested them first in tissue from a transgenic mouse model, hTau,[18] that expresses normal human tau isoforms. Importantly, when used in traditional immunohistochemistry in human tissue, all three of these antibodies labeled similar structures (Figure S9).

There was significantly more variability between tau antibodies than seen with GFAP antibodies, primarily due to the inability for DAKO to effectively penetrate the surface and bind tau (Figure 4). The inability to image DAKO-stained tau beyond the surface may be an effect of poor penetration and diffusion of the secondary antibody. Similar trends in optimal IHC protocols were observed for AT8 and HT7 in mouse tissue expressing human tau (Figure S6) and showed no labeling in mice without tau (Figure S7).

Mouse brain tissue as a model system for optimizing IHC in cleared human tissue

Optimizing IHC in human tissue is especially difficult due to the limited amount of tissue available for experimentation. Therefore, we performed IHC optimization in both mouse and human brain tissue for individual antibodies and analyzed their similarities. Surprisingly, our testing of IHC protocols for NeuN and Glut1 in human tissue showed similar changes in staining quality and depth when compared to mouse tissue (figure 5). Both human and mouse tissue showed decreases in staining quality with increasing clearing time and fixation with PFA. Epitope unmasking at 50°C for 1 hour prior to antibody incubation improved Glut1 staining in both mouse and human tissue, but had no significant effect for NeuN in human tissue and a strongly deleterious effect for NeuN in mouse tissue. It is also worth noting that this NeuN antibody appears to accumulate off-target in the human tissue, which is not observed in the mouse tissue.

The optimal protocol that allows NeuN, Glut1, and AT8-tau staining was then determined by finding the conditions that allow for the simultaneous IHC of all three antibodies in a single tissue section, and then finding the combination of conditions among those that maximizing the staining quality. It is worth noting that this was not necessarily the best protocol for each individual antibody. It is more important to have adequate staining of each epitope than to have fantastic staining of one at the cost of another. For example, using 50°C to unmask the tissue would benefit Glut1 at the cost of disrupting AT8-tau staining. The optimal protocol was then validated in 1mm thick pieces of human brain tissue, approximately 100-fold thicker than typical paraffin embedded sections. Antibodies for tau in mice expressing human tau show similar variability across conditions for the labeling of labeling tau in human tissue (figure 4). As shown in figure 3, the use of a primary antibody directly conjugated to a fluorophore greatly reduced background fluorescence over traditional primary/secondary antibody systems. Therefore, we directly conjugated three antibodies to three different fluorophores (NeuN-A568, Glut1-A488, and AT8-A647). These antibodies were used to stain tissue that was first embedded in a 4% acrylamide hydrogel , cleared for 2 days and thoroughly washed. The antibodies were incubated with the tissue for 14 days to ensure complete staining through the whole sample in both humans (figure 6) and mice (figure S10). By carefully following the optimal IHC protocol determined in this work, we were able to achieve complete penetration and simultaneous labeling of the 1 mm thick human tissue with all three antibodies. Both the Glut1-labeled vasculature and AT8-labeled tau are extremely well defined and could be easily quantitated. The NeuN reflects the same quality that it had during the troubleshooting but does not appear to be an ideal antibody for assessment of human neurons under these conditions.

Discussion

Although it is well known that alterations to IHC protocols can have detrimental effects to the staining results, many researchers accept the dogma that a universal IHC protocol exists that is robust enough to

support labeling with a wide range of antibodies. When a subset of antibodies fail in a multi-target IHC protocol, often the antibody themselves are blamed. Here, we have found that small changes to an IHC protocol can have profound effects on labeling efficiency. Rather than the antibody, our data suggests that poor staining is most often due to denaturation or blockage of the epitope. These procedural differences do not influence every antibody-antigen pair in the same way, so the optimal protocols for IHC should be determined for each individual target. Using combinations of antibodies in the same tissue may require using a protocol with conditions that enable each antibody, rather than conditions that are the best for each individual antibody. Unfortunately, as we found with the dopamine receptor 2 and GFAP IHC, a protocol may not exist to allow for both targets to be effectively stained simultaneously.

Importantly, temperature, fixation conditions, and the other conditions investigated here have greater influence the larger the tissue volume becomes. For many of the tested protocols, the difference in staining is not apparent at the surface which suggests that the use of tissue sections that are too thin does not allow for appropriate optimization. Many of the protocols we tested for NeuN or Glut1 produce some degree of labeling at the surface of the sample that would have appeared no different between samples thinner than 50 µm, despite obvious differences in staining quality at depth.

Most surprising to us, was that mouse tissue is a good model system for determining large-volume IHC protocols for human samples. However, these results show minor procedural changes can disrupt the quality of staining, so it is important that tissue preparations are identical.

IHC protocols in large volume tissue that requires clearing can take weeks or months to complete depending on the initial state and size of the tissue.[10,19] Previous studies have suggested that human tissue requires processing for longer than comparable-sized rodent tissue. Our results suggest that this is not due to intrinsic differences between human and mouse brain tissue, but rather a result of differences in the state of the tissue when clearing experiments are started. Human tissue is often stored in fixative for extended periods of time and, as our data shows, even a small increase in PFA exposure can have significant influence on IHC quality and depth. To our surprise, tissue that was delipidated for three days showed less rapid IHC penetration than tissue that was cleared for 2 days in all cases except for DAPI labeling. This suggests that samples can quickly become over cleared and lose antigenicity which may extend the amount of time previously reported as necessary for IHC. It follows that future experiments should explore labeling tissue with antibodies with even shorter or milder fixation conditions and, where possible, carried out prior to any tissue clearing procedures.

Our methodology enables rapid optimization of IHC protocols, including protocols that require tissue clearing and provides a simple path to imaging tissue blocks that are 100 times thicker than conventional tissue slices. First, a library of cleared tissue samples that were each processed using different conditions is generated that can be stored for future experiments. Then, optimal IHC conditions are determined for new antibodies within a few days (approximately 24 hours for staining, 24 hours for rinsing, 12-24 hours for refractive index matching/clearing, 3 hours to image the samples, and a similar amount of time to quantify and compare the staining quality). The variability in staining quality across protocols suggest that researchers should use this process to test how changes may affect antibodies or epitopes that they plan to study before committing many weeks or months to a procedure in larger volumes. Additionally, these results speak to the necessity for scientists to publish both conditions that improve and degrade specific antibody performance. Understanding which procedures

and antibodies are appropriate for a given sample will be essential for tissue clearing techniques to gain widespread use in human tissue. We are optimistic that our optimization process will allow researchers use these techniques to successfully label cleared human tissue, which will improve the adoption of this technique and the ability to unlock new insight into human pathology and neuroanatomy.

Materials and Methods

Human tissue samples

Three human participants with AD were selected from the Massachusetts Alzheimer's Disease Research Center. Sex, age at death, Braak staging, which hemisphere, and comorbidities are listed in Supplementary Table 1. Autopsy tissue from human brains were collected at Massachusetts General hospital, with informed consent of patients or their relatives and approval of local institutional review boards.

Mice strains

C57Bl/6J mice were used for most tissue experiments. For tissue to test IHC of tau, 10-12 month-old hTau mice (B6.Cg-Mapttm1(EGFP)Klt Tg(MAPT)8cPdav/J) that express only human tau isoforms were used. hTau knockout mice were used as controls for tau IHC experiments.

Perfusion

Mice were transcardially perfused with ice-cold 40 ml phosphate-buffered saline (PBS), followed by 40 ml 4% paraformaldehyde (PFA, Electron Microscopy Sciences). Brains were removed from the cranium and placed in 4% PFA for 48 hours at 4°C. Brains were then transferred to PBS for 24 hours at 4°C before slicing.

Tissue slicing

Brains were embedded in 4% agarose hydrogel. To do this, extracted brains were placed individually in a small petri dish and let dry slightly. The agarose solution was dissolved by boiling in a microwave, then left on the counter to cool before pouring. Agarose was poured to completely cover the top of the brain, which allows it to provide a solid support to prevent deformation during cutting. A block of agarose containing the brain was placed in a vibratome (VT1000S vibrating blade microtome, Leica, Wetzlar, Germany) then cut into 500 or 1000 µm coronal or sagittal slices. Each slice was then removed from the agarose through gentle manipulation with blunt forceps or paintbrushes before crosslinking.

Tissue hydrogel crosslinking

Each slice was incubated with a hydrogel crosslinking solution for 1 day at 4°C to let the molecules diffuse through the tissue. Solutions should be kept cold before and after the addition of VA-044 to prevent premature initiation of polymerization. Different crosslinking solutions were used to determine the effect of including PFA on IHC. *Crosslinking solution 1*: PBS with 4% (wt/vol) acrylamide (Sigma-Aldrich, St. Louis, MO) and 0.25% (wt/vol) VA-044 thermal polymerization initiator (Fisher Scientific, Pittsburgh, PA). *Crosslinking solution 2*: PBS with 4% (wt/vol) acrylamide, 0.25% (wt/vol) VA-044 thermal polymerization initiator, and 4% PFA. After incubation with the crosslinking solution for 1 day, the tissue was left in solution and placed in vacuum at 37°C for 3 hours. After polymerization with X-CLARITY polymerization system (Logos Biosystems, South Korea), the slices were rinsed with 50 ml PBS three

times over 3 hours. Each slice was then cut into small pieces with width and length at least twice the thickness. This was done to increase the number of conditions that could be tested with small amounts of tissue.

Delipidation

After hydrogel crosslinking, the tissue was placed in a delipidation solution (SDS 200 mM, Sodium sulfite 20mM, Sodium Borate 20mM, Sodium Hydroxide to pH 8.5-9. Filtered if necessary) at 37°C for different amounts of time (1, 2, or 3 days), to determine the effect of delipidation in IHC. After delipidation, the brain slices were rinsed with 50 ml PBST (PBS with 0.2% Triton X-100, Thermo Fisher Scientific) five times over 1 day.

Pre-immunohistochemistry tissue processing

Different conditions were tested at this step to determine their influence on immunohistochemistry. Each tissue section was tested using only one of the following conditions. *Baseline:* Tissue was left at 4°C in PBST. *50°C Condition:* Tissue was heated to 50°C for 1 hour in PBST. *Glycine:* Tissue was incubated with 0.1 M Glycine at 4°C for 12-18 hours. *Glycerol:* Tissue was placed in a low osmolarity solution of 80% glycerol/20% water for 12-18 hours. *Blocking:* Tissue was placed in 5% BSA in PBS for 12-18 hours

Immunohistochemistry

- The following antibodies were purchased then stored according to the vendors specifications: NeuN antibody conjugated to Alexa Fluor 568 (Abcam, Ab207282).
- GFAP antibody unconjugated (Abcam, ab16997) and conjugated to Alexa Fluor 488 (Thermo Fisher, 53-9892-82).
- Glut1 antibody conjugated to Alexa Fluor 488 (Sigma-Aldrich, 07-1401-AF488).
- Phospho-Tau antibody AT8 conjugated to biotin (Thermo Fisher, MN1020B).
- Tau monoclonal antibody HT7 conjugated to Alexa Fluor 647 (Thermo Fisher, 51-5916-42).
- DAKO tau antibody unconjugated (Agilent, A0024).
- Secondary antibody Goat Anti-Rabbit IgG H&L conjugated to Alexa Fluor 405 (Abcam, ab175652) and Alexa Fluor 647 (ab150079).
- Streptavidin conjugated to Alexa Fluor 568 (Thermo Fisher, S11226).

Each brain slice was placed in a 2ml Eppendorf tube (or similar vessel) that could hold the slice so its large, flat sides could be exposed to solution. PBST was added to just cover the top of the samples (~300 µl). 1-5 µl of stock antibody solution was added, depending on the concentration of the stock. The final concentration of each antibody in solution was 5 µg/ml. Fluorophores or host species were chosen so multiple different antibodies could be tested at the same time in a single slice of tissue. The tissue was then incubated with the antibodies at 4°C or room temperature for 18 hours. The tissue was then rinsed in PBST 3x 50ml overnight (18-24 hours) at room temperature.

IHC of human microtome sections

Prior to preparation of cleared tissue volumes, fresh/frozen human samples were tested for the presence of AT8, HT7, and DAKO. Microtome sections were fixed in 4% PFA for 15 minutes, rinsed in Tris-buffered saline (TBS) three times, then blocked in TBS with 5% bovine serum albumin. Primary antibodies were incubated at a concentration of 1:500 overnight. Tissue was rinsed in TBS 3x, then

incubated in secondaries at room temperature for 60 minutes, and rinsed in TBS 3x. Immumount was then used to seal the tissue prior to imaging.

Refractive index matching

The samples were incubated with 80% glycerol, 15% DI water, 5% PBS (RI-matching solution) for at least 3 hours at RT with gentle shaking. The RI-matching solution was then replaced with fresh solution and left to incubate for at least 3 more hours before imaging. Samples were stable stored in this solution at room temperature and could be re-imaged for at least 3 months.

Imaging

Samples were imaged using Olympus Inverted Confocal FV3000 with a 10x objective except for samples using dopamine receptor antibodies which were imaged using the Zeiss Lightsheet Z.1. Image Z-stacks were then reconstructed and visualized using Imaris microscopy image analysis softwhere.

Post-imaging analysis

Imaris software was used to assess the staining quality score. First, the distribution of fluorescence values across all slices in the z-stack were normalized. Then, a rolling ball algorithm was applied to define the edges of fluorescent shapes with signal intensity greater than background by a threshold value. The area within each slice of a z-stack that contained staining above this threshold was then divided by the maximum across all tissue stained with that fluorophore to determine the staining quality throughout the tissue. This metric was only applied to stains like NeuN or Glut1 in the cortex where we can make the assumption that there is a uniform and consistent distribution of these cells across sections.

Data availability

Data will be provided upon reasonable request to the corresponding author.

Code availability

All Matlab code used to quantify data will be provided upon reasonable request to the corresponding author.

Acknowledgements

This work was supported by the NIH/NIA-K99AG068602 (T.J.Z.) and the Harrison Gardner, Jr. Award (T.J.Z)

We would like to thank Massachusetts General Hospital Center for comparative Medicine and Analiese Fernandes for help with animal husbandry and care. We would also like to thank the Harvard Center for Biological Imaging including Christian Hellriegal for the use of their imaging facility and helpful conversations. Autopsy tissue from human brains were collected at Massachusetts General hospital, with informed consent of patients or their relatives and approval of local institutional review boards.

Author Information

Affiliations

Department of Neurology, Massachusetts General Hospital, Harvard Medical School, Boston, MA, USA

Theodore J. Zwang, Rachel E. Bennett, Maria Lysandrou, Benjamin Woost, Bradley T. Hyman

Harvard Medical School, Boston, MA, USA

Theodore J. Zwang, Rachel E. Bennett, Bradley T. Hyman

Massachusetts Alzheimer's Disease Research Center, Charlestown, MA, USA

Theodore J. Zwang, Rachel E. Bennett, Bradley T. Hyman

Department of Molecular and Cellular Biology and Harvard Center for Biological Imaging, Harvard University, Cambridge, MA, USA

Douglas S. Richardson

Department of Chemistry and Chemical Biology, Harvard University, Cambridge, MA, USA

Charles M. Lieber

Department of Chemical Engineering, Stanford University, Stanford, CA, USA

Anqi Zhang

Contributions

T.J.Z. designed the study and performed most of the experiments and analysis. T.J.Z., A.Z., C.M.L, R.E.B., D.C.R. and B.T.H. conceived of experiments. T.J.Z., M.L., R.E.B., and B.W. performed tissue collection, preparation, staining, and imaging. All authors discussed the results and commented on the manuscript text.

Corresponding author

Correspondence to Theodore J. Zwang (tzwang@mgh.harvard.edu)

Competing Interests

The authors declare no competing interests.

References

1) Ueda, H.R., Ertürk, A., Chung, K. *et al.* Tissue clearing and its applications in neuroscience. *Nat Rev Neurosci* **21,** 61–79 (2020).
2) Richardson DS, Guan W, Matsumoto K, et al. TISSUE CLEARING. *Nat Rev Methods Primers*. **1**, 84 (2021)
3) Kim SW, Roh J, Park CS. Immunohistochemistry for Pathologists: Protocols, Pitfalls, and Tips. *J Pathol Transl Med*. **50**, 411-418 (2016)
4) Murray E, Cho JH, Goodwin D, et al. Simple, Scalable Proteomic Imaging for High-Dimensional Profiling of Intact Systems. *Cell*. **163**, 1500-1514. (2015)
5) Yun, D.H., Park, Y-G., Cho, J.H. *et al.* Ultrafast immunostaining of organ-scale tissues for scalable proteomic phenotyping *BioRxiv* doi: https://doi.org/10.1101/660373 (2019)

6) Na, M., Kim, K., Lim, H. R., Ha, C. M. & Chang, S. Rapid immunostaining method for three-dimensional volume imaging of biological tissues by magnetic force-induced focusing of the electric field. Brain Struct. Funct. 226, 297–309 (2021).
7) Dwyer, J., Ramirez, M. D., Katz, P. S., Karlstrom, R. O. & Bergan, J. Accelerated clearing and molecular labeling of biological tissues using magnetohydrodynamic force. Sci. Rep. 11, 16462 (2021)
8) Marina, S., Luca P., Niamh b. *et al.* Comparison of Different Tissue Clearing Methods for Three-Dimensional Reconstruction of Human Brain Cellular Anatomy Using Advanced Imaging Techniques. *Front. Neuroanat.* **15** (2021)
9) Lai, H.M., Liu, A.K.L., Ng, H.H.M. *et al.* Next generation histology methods for three-dimensional imaging of fresh and archival human brain tissues. *Nat Commun* **9,** 1066 (2018)
10) Susaki, E.A., Shimizu, C., Kuno, A. *et al.* Versatile whole-organ/body staining and imaging based on electrolyte-gel properties of biological tissues. *Nat Commun* **11,** 1982 (2020)
11) Matos LL, Trufelli DC, de Matos MG, da Silva Pinhal MA. Immunohistochemistry as an important tool in biomarkers detection and clinical practice. *Biomark Insights*. **5**, 9-20 (2010)
12) Zhao et al., Cellular and Molecular Probing of Intact Human Organs. *Cell*. 2020
13) Richardson DS, Lichtman JW. Clarifying Tissue Clearing. Cell. **162**, 246-257 (2015)
14) Shi S-R, Shi Y, Taylor CR. Antigen Retrieval Immunohistochemistry: Review and Future Prospects in Research and Diagnosis over Two Decades*. Journal of Histochemistry & Cytochemistry*. **59**, 13-32 (2011)
15) Wassie, A.T., Zhao, Y. & Boyden, E.S. Expansion microscopy: principles and uses in biological research. *Nat Methods* **16**, 33–41 (2019)
16) Park, YG., Sohn, C., Chen, R. *et al.* Protection of tissue physicochemical properties using polyfunctional crosslinkers. *Nat Biotechnol* **37,** 73–83 (2019)
17) Muratov EN, Bajorath J, Sheridan RP et al. QSAR without borders. *Chem Soc Rev.* **49**, 3525-3564 (2020)
18) Andorfer C, Kress Y, Espinoza M *et al*. Hyperphosphorylation and aggregation of tau in mice expressing normal human tau isoforms. *J Neurochem*. **86**, 582-90 (2003)
19) Ueda, H.R., Dodt, H.-U., Osten, P. et al. Whole-Brain Profiling of Cells and Circuits in Mammals by Tissue Clearing and Light-Sheet Microscopy. *Neuron.* **106**, 369-387 (2020)

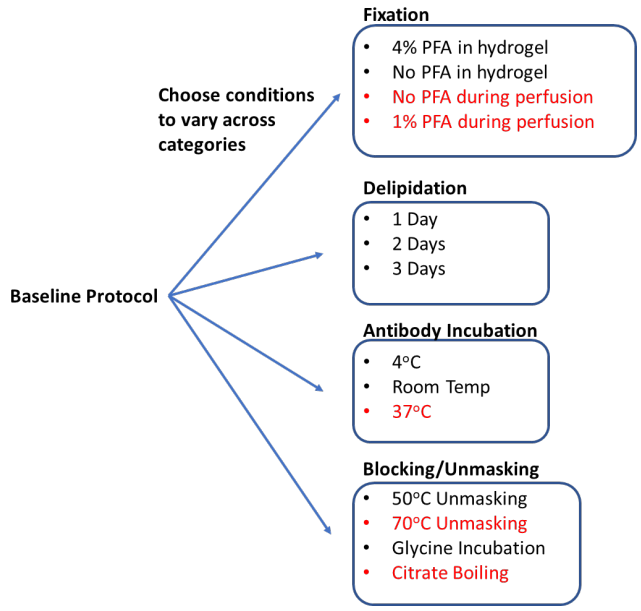

Scheme 1. Process for generating a library of tissue prepared with different protocols. Start with a baseline protocol (see Methods). Choose conditions to test that can be separated into categories believed to influence staining quality. Vary only one or two conditions from the baseline, to isolate the effect of the condition change on IHC. Comparisons between protocols allow for inference about the optimal combinations of conditions or extrapolation to predict the influence of further changes. Stored library of cleared tissues then allows for rapid antibody testing to quickly determine optimal IHC conditions. We consistently found conditions in red to have exclusively negative effects on IHC or tissue integrity, so they were excluded from testing with most antibodies.

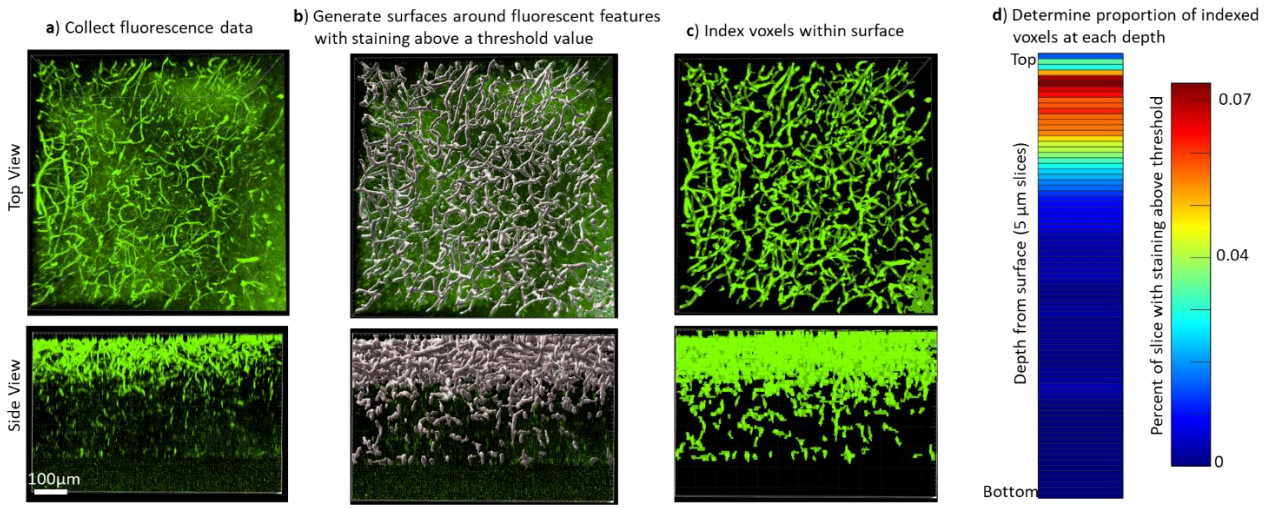

Scheme 2. Quantifying the staining quality for comparison across protocols and antibodies. IHC quality comparisons can be difficult to determine by eye due to differences in fluorescence intensity and background, as well as the many ways that software can modify the visual representation of data, so we created a pipeline to quickly quantify staining quality in a way that allows rapid comparison. **a** First, a confocal or lightsheet microscope is used to image a Z-stack throughout the entire thickness of the

sample. All imaging parameters are kept identical for a given antibody/fluorophore to allow for comparison between protocols. **b** Fluorescence values were normalized across the sample, then a rolling-ball algorithm was used in Imaris software to generate surfaces around fluorescent features with intensity above a threshold value. **c** The voxels within the surface were indexed to define the array of voxels with and without staining that could then be analyzed in Matlab. **d** The staining quality was then visualized by plotting the ratio of voxels with staining over the total number of voxels in a plane at that depth in the image. A higher proportion of indexed voxels represents better staining quality. This representation can also be used to provide visual representation of reproducibility (Fig S1, S2) Staining quality can be further simplified to one dimension for easy comparison (Fig S3).

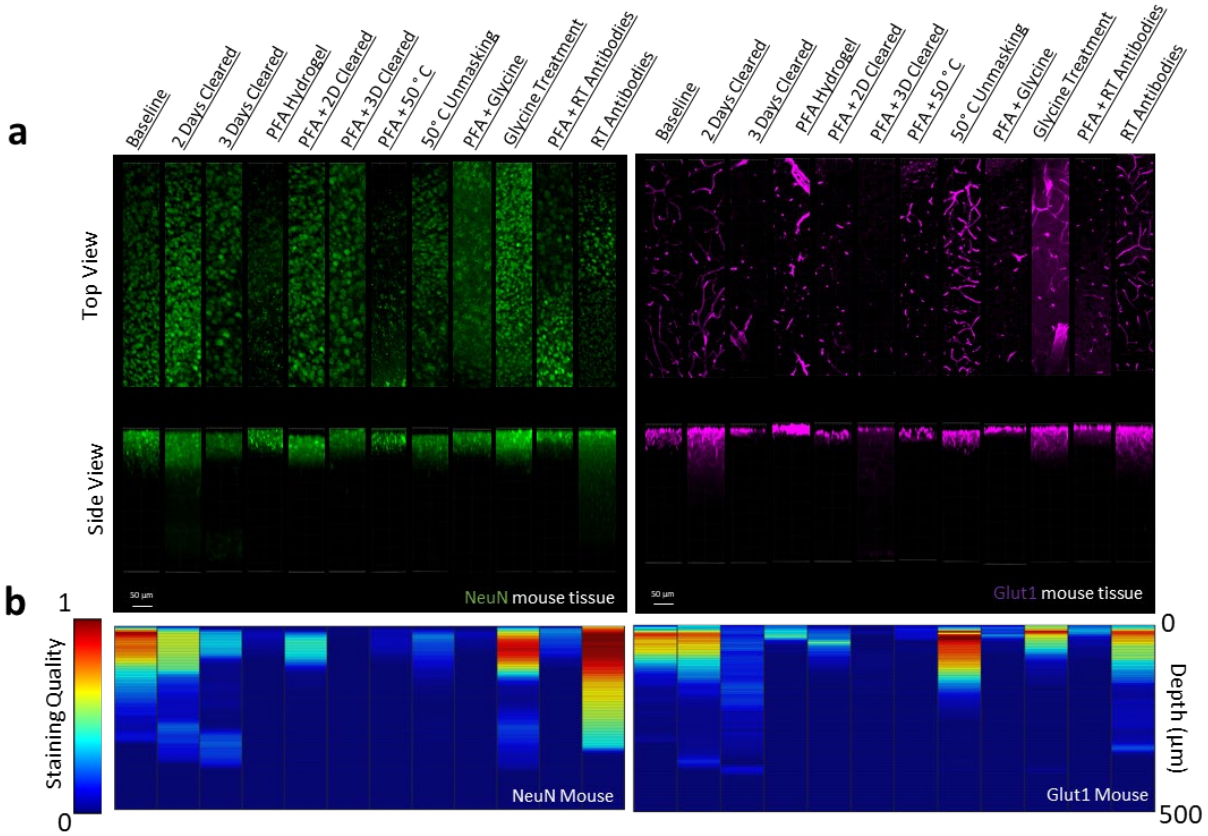

Figure 1. Influence of common conditions on immunohistochemistry in mouse brain tissue. a Representative maximum intensity projection views from the top and side of 500µm thick, 5mm wide tissue sections. C57Bl/6J mouse isocortex was processed, stained, and imaged simultaneously with NeuN (green, left panels) and Glut1 (purple, right panels). **b** Quantitative comparison of immunohistochemistry labeling across conditions. A rolling-ball subtraction was used to determine the area with signal-to-noise above cut-off for every image plane in the Z-stack. The proportion of indexed voxels in each plane was then divided by the maximum value across all conditions to generate a normalized staining quality score, which allows for quick visual assessment of staining quality differences with depth and between conditions.

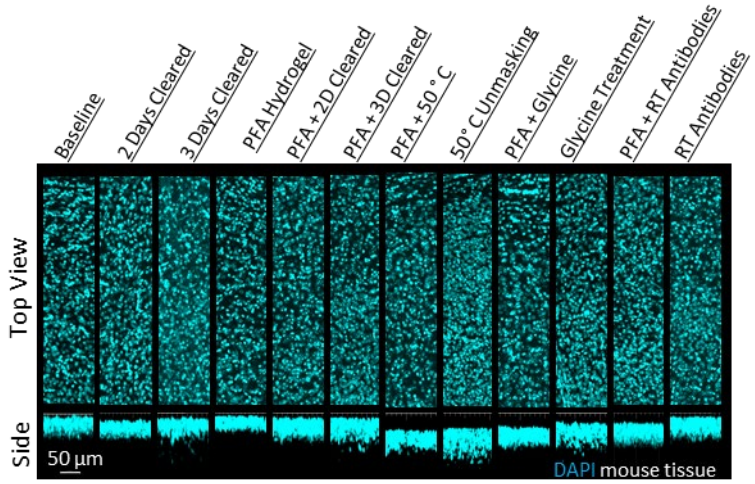

Figure 2. Influence of common conditions on DAPI staining. Representative maximum intensity projection views from the top and side of 500µm thick, 5mm wide tissue sections of C57Bl/6J mouse isocortex stained with DAPI.

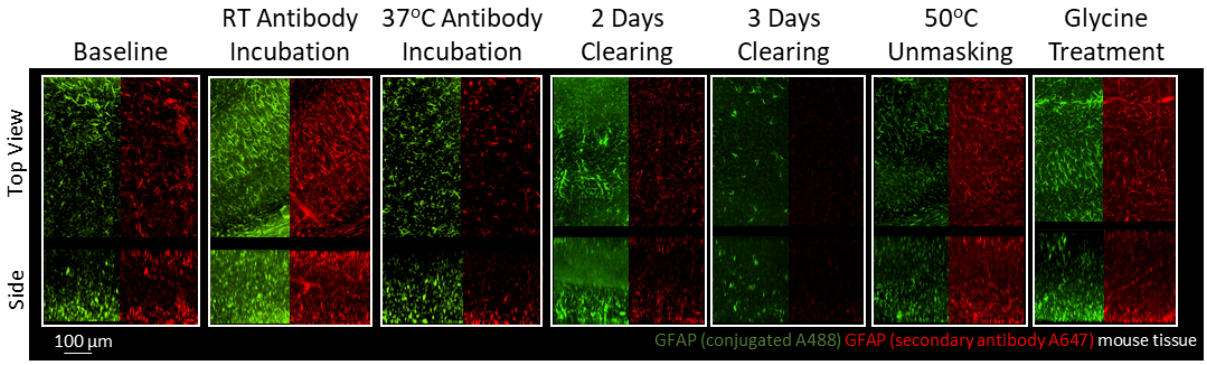

Figure 3. Immunohistochemistry of two different antibodies for GFAP. Representative maximum intensity projection views from the top and side of 500µm thick, 5mm wide tissue sections of C57Bl/6J mouse isocortex stained with two different antibodies for GFAP. Monoclonal GA5 conjugated to Alexa Fluor 488 (green) was stained and imaged in the same tissue as a polyclonal antibody using a goat anti-rabbit secondary conjugated to Alexa Fluor 647 (red). Other protocols show no significant labeling (S4).

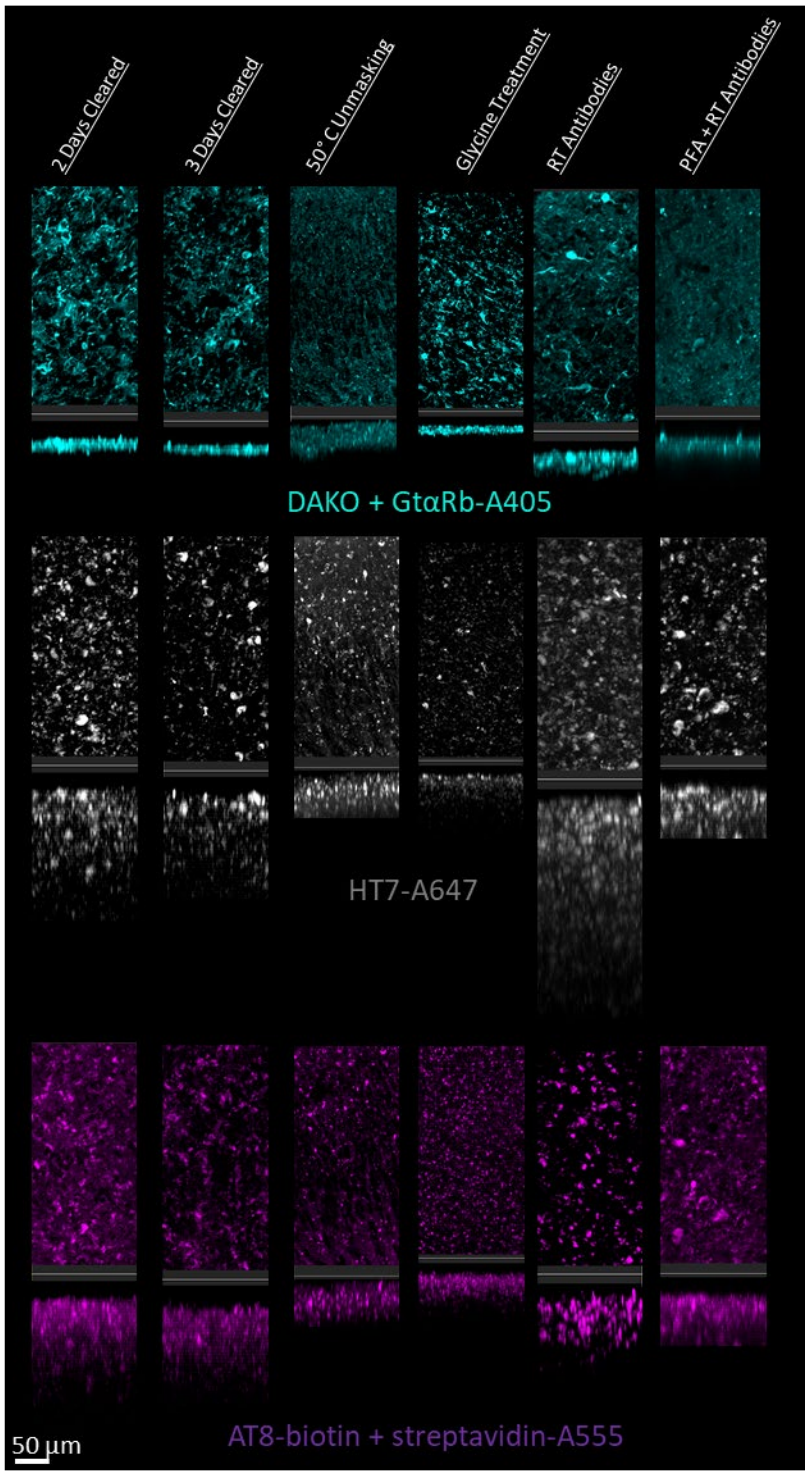

Figure 4. Tau immunohistochemistry in cleared human tissue. Representative maximum intensity projection views from the top and side of 500µm thick, 5mm wide tissue sections from frozen human tissue samples. Other protocols showed worse staining quality (Fig. S8)

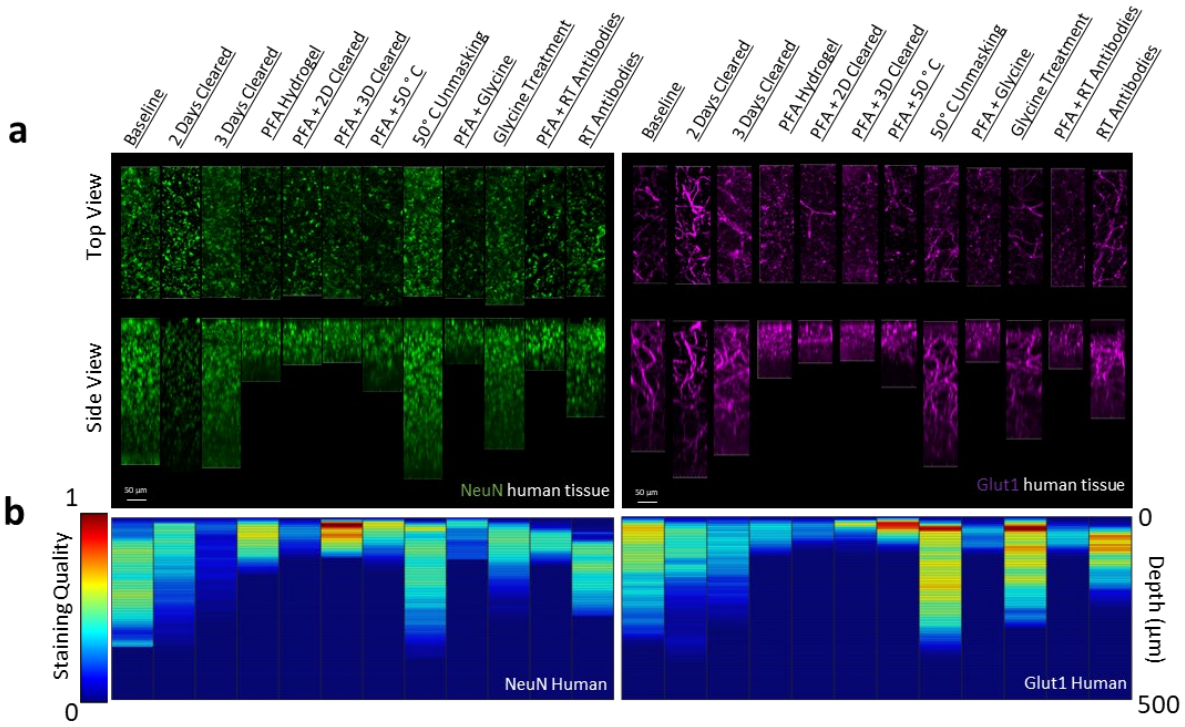

Figure 5. Influence of common conditions on immunohistochemistry in human brain tissue. a Representative maximum intensity projection views from the top and side of 500µm thick, 5mm wide tissue sections. Tissue was processed, stained, and imaged simultaneously with NeuN (green, left panels) and Glut1 (purple, right panels). **b** Quantitative comparison of immunohistochemistry labeling across conditions. A rolling-ball subtraction was used to determine the area with signal-to-noise above cut-off for every image plane in the Z-stack. The area in each plane was then divided by the maximum value across all conditions to provide a staining quality score, which allows for quick visual assessment of staining quality differences with depth and between conditions.

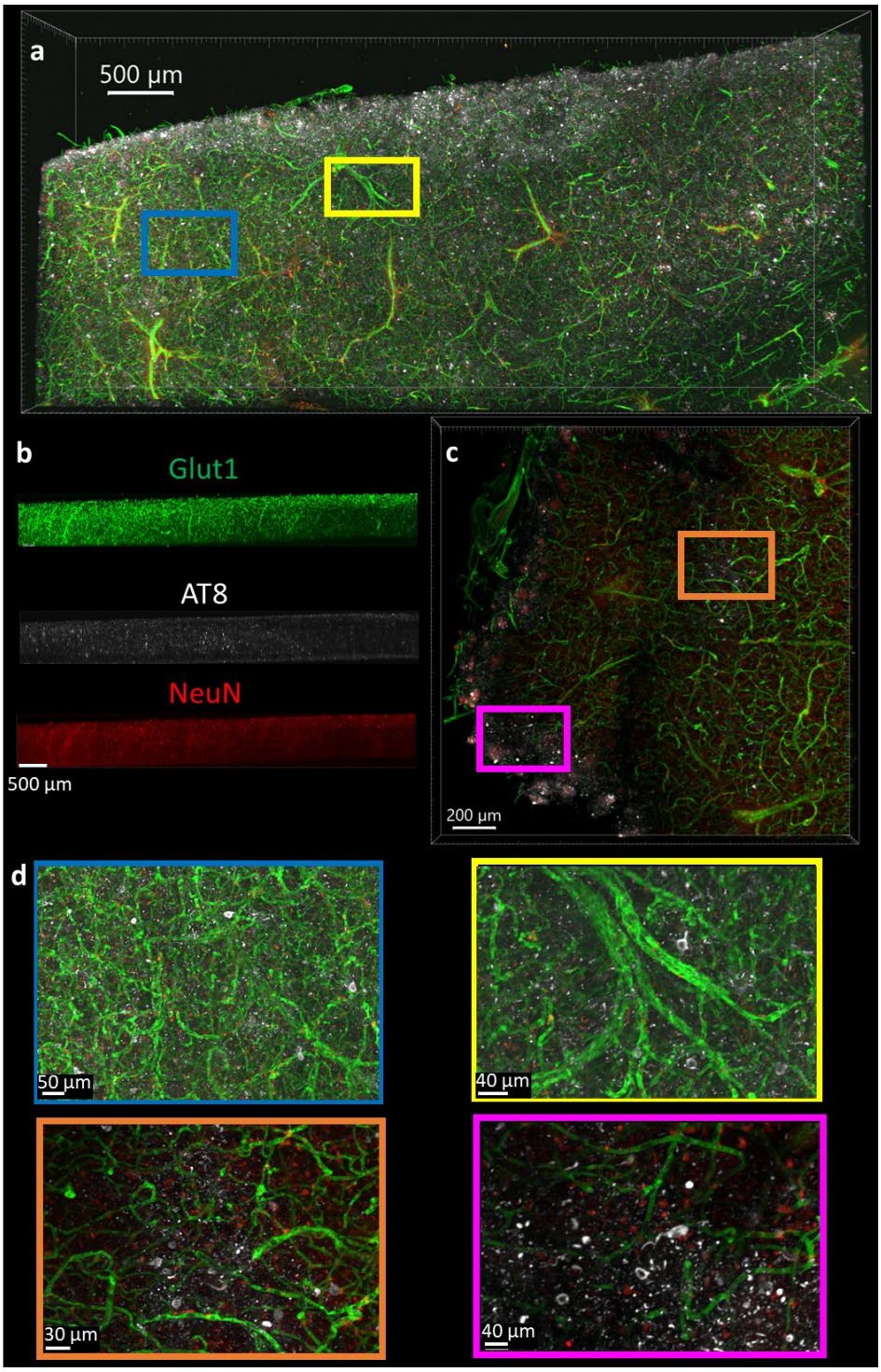

Figure 6. Immunohistochemistry in 1 mm thick human tissue. The tissue was crosslinked without PFA, cleared for 2 days, rinsed, then the antibodies NeuN-A568 (Red), Glut1-A488 (Green), and AT8-A647 (White) were incubated with the tissue for 14 days. **a** Top-down view of fluorescence from 1mm section human brain. **b** Side view of each antibody fluorescence through entire section depth. **c** A 200 µm virtual section of human tissue, from a 1mm thick sample. **d** Zoomed-in regions from the full images show AT8-labeled tau tangles are present at multiple locations throughout the human brain sections.

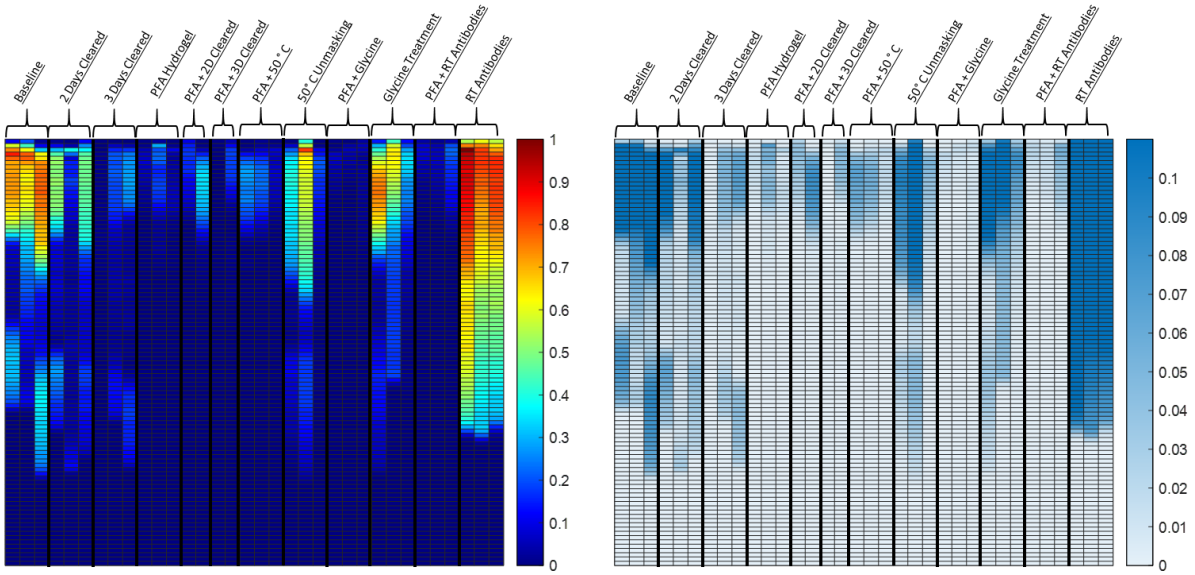

Figure S1. Reproducibility of NeuN immunohistochemistry in mouse brain tissue. Quantitative comparison of immunohistochemistry labeling across conditions. N = 3 independently prepared tissue sections from different mice for each condition. All conditions were tested with one section each from the same three mice. A rolling-ball subtraction was used to determine the area with signal-to-noise above cut-off for every image plane in the Z-stack. (Left) The area in each plane was then divided by the maximum value across all conditions to provide a staining quality score, which allows for quick visual assessment of staining quality differences with depth and between conditions. (Right) The area of each slice in the z-stack with fluorescence above the threshold value.

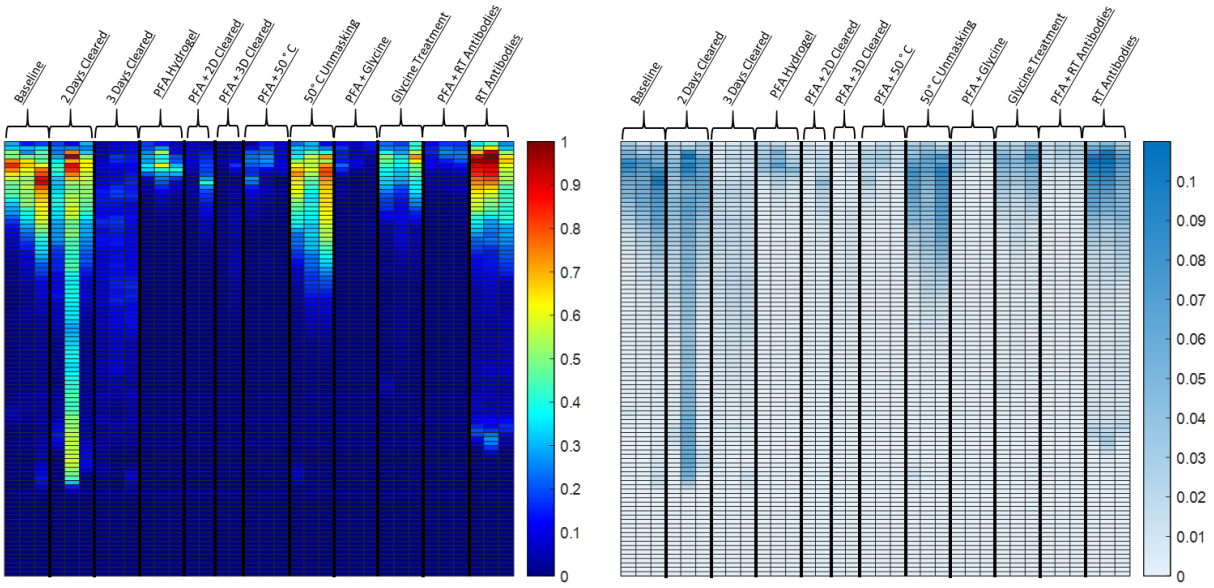

Figure S2. Reproducibility of Glut1 immunohistochemistry in mouse brain tissue Quantitative comparison of immunohistochemistry labeling across conditions. N = 3 independently prepared tissue sections from different mice for each condition. All conditions were tested with one section each from the same three mice. with each condition having every condition having . A rolling-ball subtraction was used to determine the area with signal-to-noise above cut-off for every image plane in the Z-stack. (Left) The area in each plane was then divided by the maximum value across all conditions to provide a staining quality score, which allows for quick visual assessment of staining quality differences with depth and between conditions. (Right) The area of each slice in the z-stack with fluorescence above the threshold value.

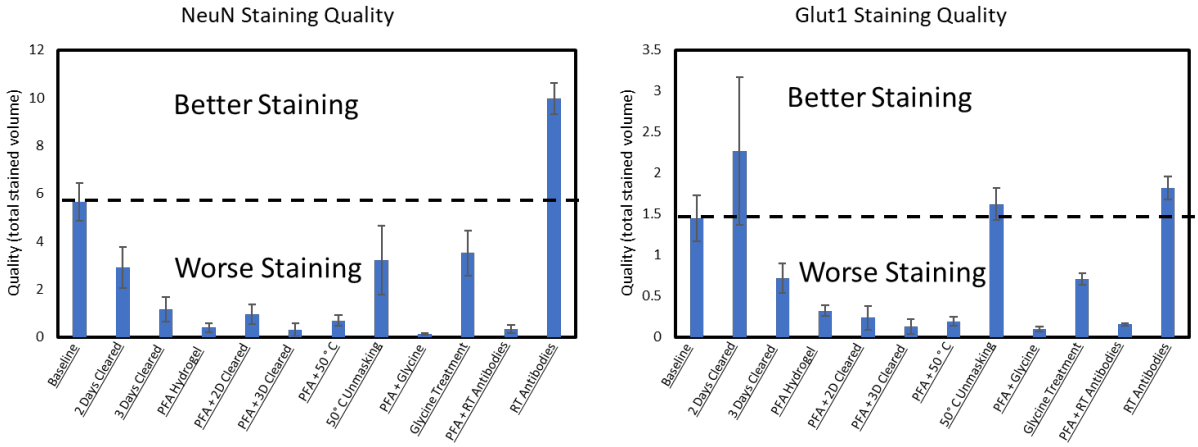

Figure S3. Reducing comparison of staining quality to one-dimension. Quantitative comparison of immunohistochemistry labeling across conditions. A rolling-ball subtraction was used to determine the area with signal-to-noise above cut-off for every image plane in the Z-stack. The total area in each plane with fluorescence above the threshold value was them summed to reduce the dimensionality of comparison and allow for a comparison between conditions with a single number as the figure of merit.

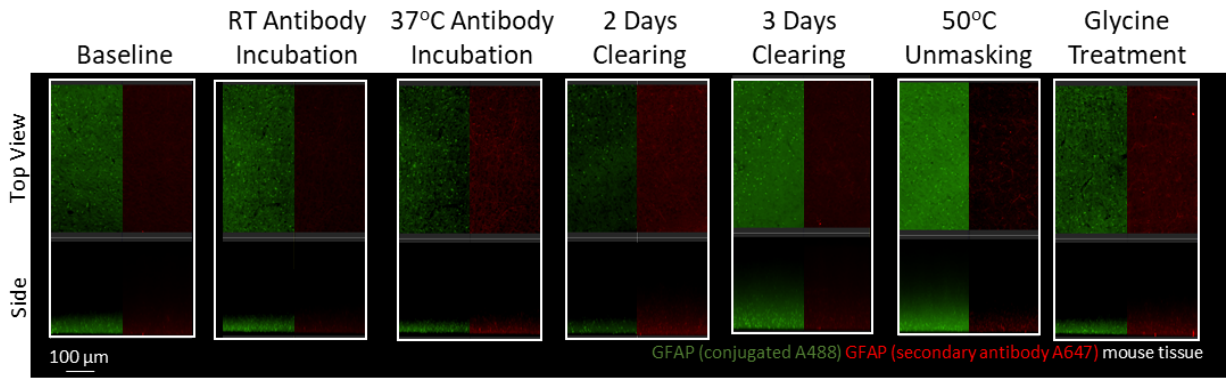

Figure S4. Immunohistochemistry with GFAP antibodies in with PFA-hydrogelled mouse brain tissue. Representative maximum intensity projection views from the top and side of 500µm thick, 5mm wide tissue sections of C57Bl/6J mouse isocortex stained with two different antibodies for GFAP. Monoclonal GA5 conjugated to Alexa Fluor 488 (green) was stained and imaged in the same tissue as a polyclonal antibody using a goat anti-rabbit secondary conjugated to Alexa Fluor 647 (red).

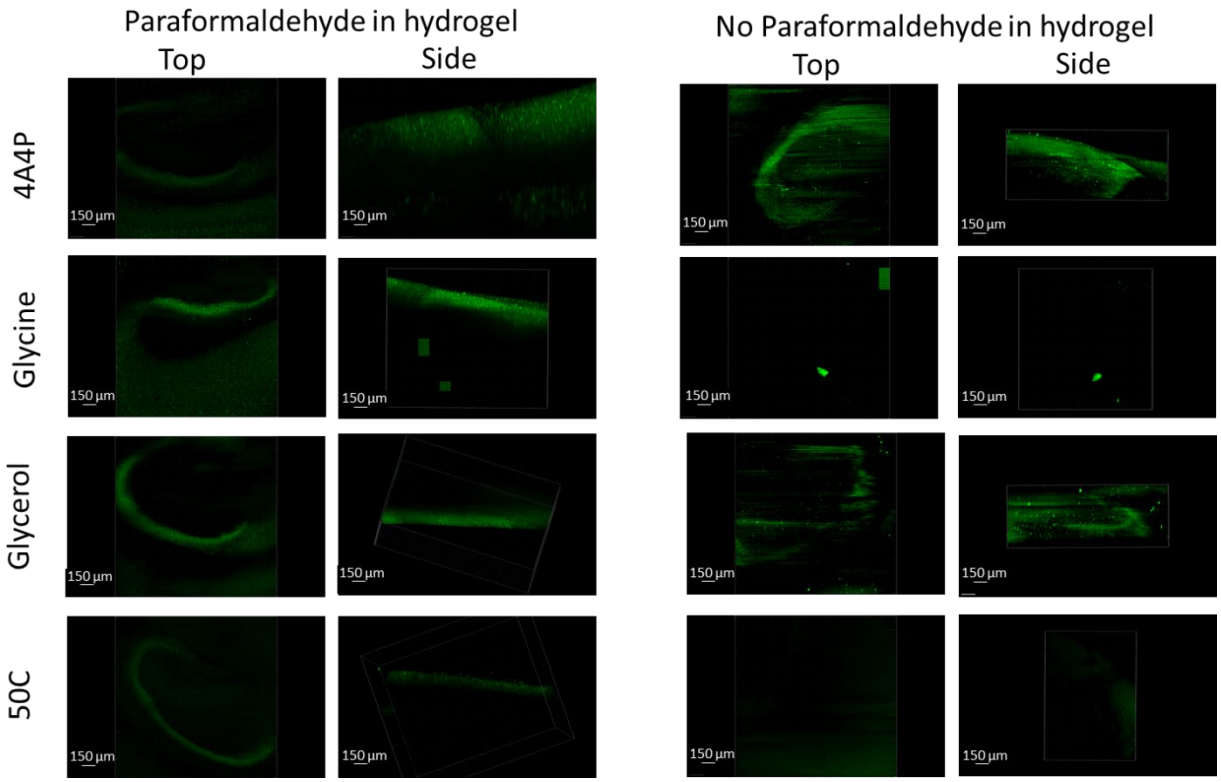

Figure S5. Immunohistochemistry of dopamine receptor 2 in mouse brain tissue. Representative maximum intensity projection views from the top and side of 1mm thick sagittal slices of C57Bl/6J mouse brain. Dopamine receptor 2 (green) shows significantly better preserved fluorescence in both the cortex and hippocampus when the tissue is prepared with PFA in hydrogel.

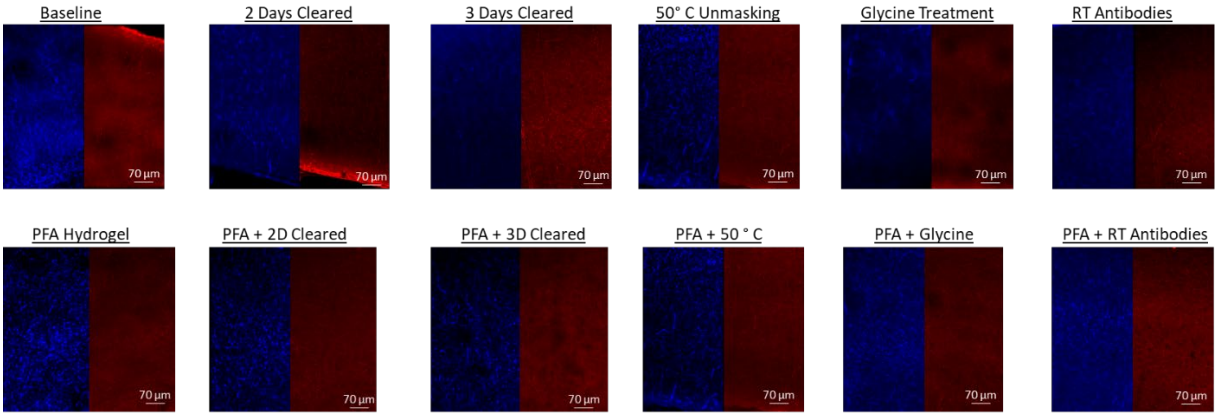

Figure S6 AT8 and HT7 immunohistochemistry in mouse tissue expressing human tau (Htau). Representative maximum intensity projection views from the top of 500µm thick, 5mm wide tissue sections of HTau mouse isocortex AT8 (Blue) and HT7 (Red) show labeling of tau in mice expressing human tau in the same conditions that show staining in human tissue.

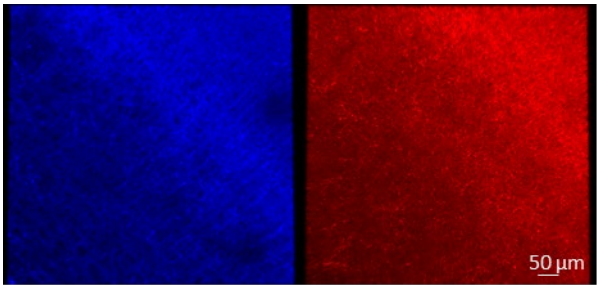

Figure S7 AT8 and HT7 immunohistochemistry in tau knockout mice (Htau KO). Representative maximum intensity projection views from the top of 500µm thick, 5mm wide tissue sections of Htau knockout mouse isocortex. AT8 (Blue) and HT7 (Red) show no labeling of tau in knockout mice using the same baseline conditions where they show labeling in Htau mice expressing human tau.

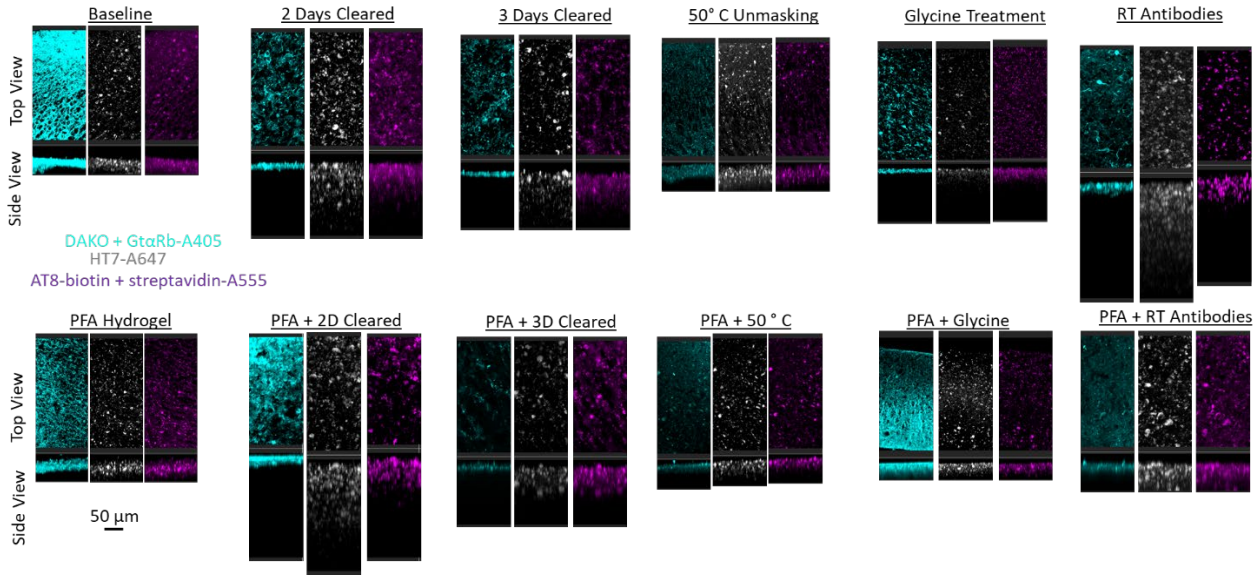

Figure S8 Additional Dako, AT8, and HT7 Tau immunohistochemistry conditions in human brain tissue
Representative maximum intensity projection views from the top and side of 500µm thick, 5mm wide tissue sections from frozen human tissue samples.

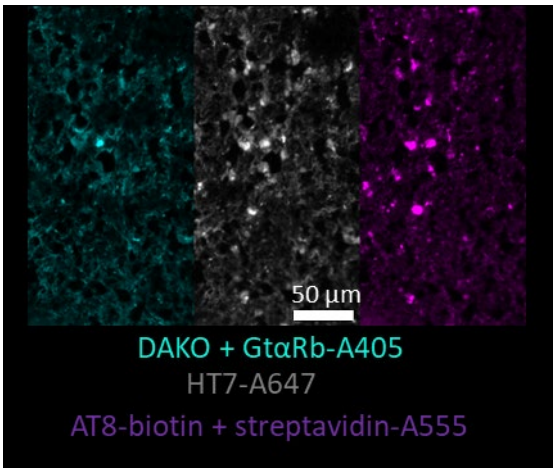

Figure S9 Representative microtome images taken from the human tissue prior to staining. Human tissue was stained with Dako, AT8, and HT7 to confirm the presence of their target Tau prior to testing large volume IHC conditions.

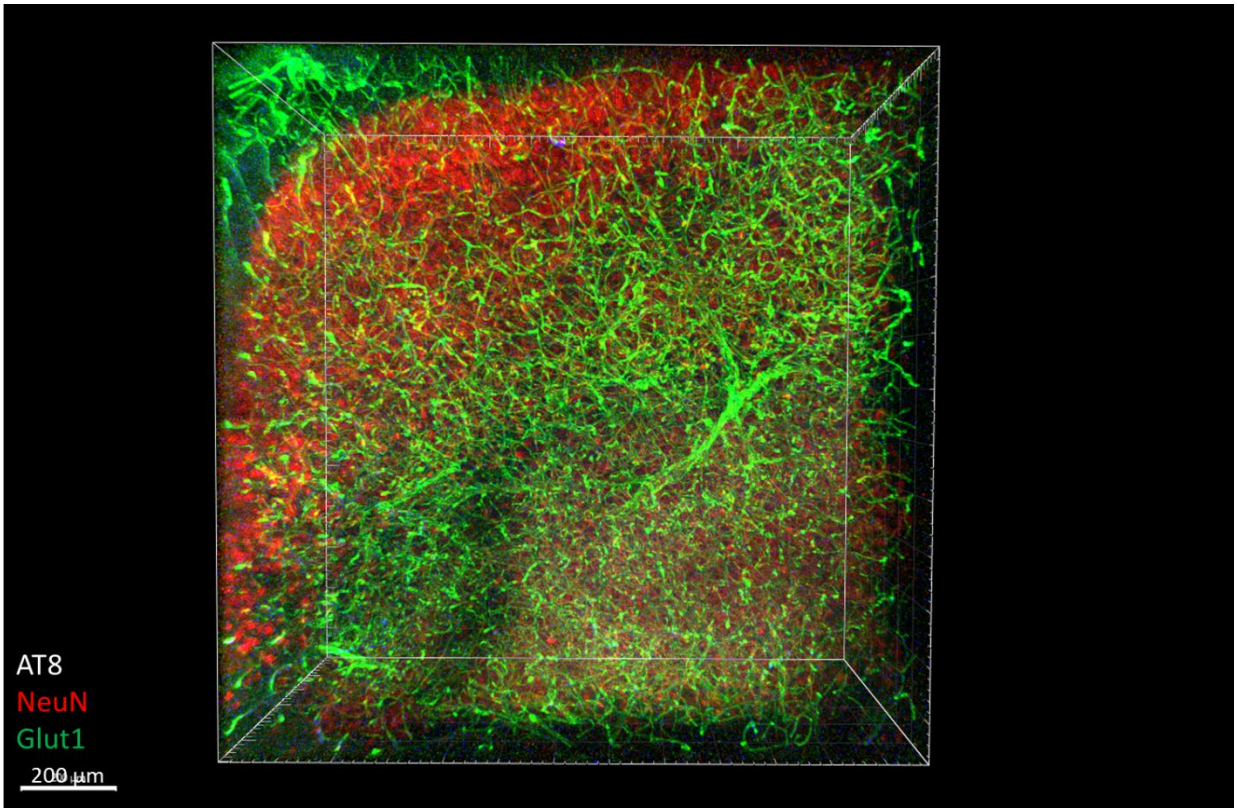

Figure S10 Immunohistochemistry in 1mm mouse tissue The tissue was crosslinked without PFA, cleared for 2 days, rinsed, then the antibodies NeuN-A568 (Red), Glut1-A488 (Green), and AT8-A647 (Blue) were incubated with the tissue for 14 days. A small section of the total stained tissue was imaged and shows complete staining throughout the entire thickness of the sample.

Sample Number	Sex	Age at Death	Braak Staging	Hemisphere	Comorbidities
1 (1581)	M	89	VI	Frozen Left	CVD and CAA
2 (1762)	F	71	VI	Frozen Right	CVD and CAA
3 (2620)	M	52	N/A	Frozen Right	N/A

Supplementary table 1. Demographic and characteristics of all subjects used in this study including sex (M = Male ; F = Female), Age at death, Braak stage, Hemisphere, CerebroVascular Disease (CVD), and Cerebral Amyloid Angiopathy (CAA).